N-Methylated Peptide Inhibitors of β-Amyloid Aggregation and Toxicity. Optimization of the Inhibitor Structure†

Nicoleta Kokkoni,‡ Kelvin Stott,§ Hozefa Amijee,‡,§ Jody M. Mason,‡ and Andrew J. Doig*,‡

Manchester Interdisciplinary Biocentre, The University of Manchester, 131 Princess Street, Manchester, M1 7DN, United Kingdom, and Senexis Limited, Babraham Research Campus, Cambridge CB2 4AT, United Kingdom

Received April 28, 2006; Revised Manuscript Received June 14, 2006

ABSTRACT: The key pathogenic event in the onset of Alzheimer's disease (AD) is believed to be the aggregation of the β-amyloid (Aβ) peptide into toxic oligomers. Molecules that interfere with this process may therefore act as therapeutic agents for the treatment of AD. N-Methylated peptides (meptides) are a general class of peptide aggregation inhibitors that act by binding to one face of the aggregating peptide but are unable to hydrogen bond on the other face, because of the *N*-methyl group replacing a backbone NH group. Here, we optimize the structure of meptide inhibitors of Aβ aggregation, starting with the KLVFF sequence that is known to bind to Aβ. We varied the meptide length, N-methylation sites, acetylation, and amidation of the N and C termini, side-chain identity, and chirality, via five compound libraries. Inhibitor activity was tested by thioflavin T binding, affinity chromatography, electron microscopy, and an 3-(4,5-dimethylthiazol-2-yl)-2,5-diphenyltetrazolium bromide toxicity assay. We found that inhibitors should have all D chirality, have a free N terminus but an amidated C terminus, and have large, branched hydrophobic side chains at positions 1−4, while the side chain at position 5 was less important. A single *N*-methyl group was necessary and sufficient. The most active compound, D-[(chGly)-(Tyr)-(chGly)-(chGly)-(mLeu)]-NH_2, was more active than all previously reported peptide inhibitors. Its related non-N-methylated analogues were insoluble and toxic.

Alzheimer's disease (AD)[1] is the most common form of senile dementia, affecting more than 15 million people worldwide. With an increased life expectancy and aging population, this number is set to rise considerably. At least 20 diseases are caused by proteins or peptides folding incorrectly and aggregating into fibrils or plaques, including AD, type-II diabetes, Parkinson's disease, Huntington's disease, and the spongiform encephalopathies (*1*). They accumulate either intra- or intercellularly in a variety of organs, including the liver, spleen, and, most importantly, the brain, causing severe neurological disorders. The aggregates are often in the form of regular amyloid fibrils. Amyloid is rich in β-sheet structure, with hydrogen bonding between monomers parallel to the fibril axis, leading to fibrils of indefinite length. The best studied amyloid-based disease is AD, characterized pathologically by abnormally high levels of brain lesions (senile plaques) and neurofibrillary tangles in dead and dying neurons and by elevated numbers of amyloid deposits in the walls of cerebral blood vessels (*2*). The major component of senile plaques is a small peptide of 39−43 amino acids called β-amyloid (Aβ). Aβ(1−40) is the most prevelant species, while Aβ(1−42) is more toxic; other lengths are rare. Aβ is produced through endoproteolysis of the amyloid precursor protein. Compelling evidence indicates that factors that increase the production of Aβ, particularly its more amyloidogenic variants, or that facilitate deposition or inhibit elimination of amyloid deposits cause AD or are risk factors for the disease (*3*).

Controversy has raged over whether the fibrils are an epiphenomenon linked to disease or whether fibril formation causes disease (*4*). For example, while many mutations in the Aβ precursor protein gene are linked to premature onset of AD, the amount of amyloid deposited in the brain does not correlate to severity. A resolution of this apparent paradox from in vitro and in vivo evidence is that soluble, oligomeric forms on Aβ have potent neurotoxic activity and are the primary causes of neuronal injury and cell death occurring in AD (*5*, *6*).

Numerous groups are developing treatments designed to block various key steps in the amyloidosis process. Specific therapeutic strategies currently being pursued include (*7*−*9*) (1) inhibiting the expression of the amyloidogenic protein or stabilizing its native form using small organic ligands, (2) inhibiting the release of the amyloidogenic peptide from its parent protein using protease inhibitors, (3) inhibiting the aggregation of the protein or peptide directly using small ligands or indirectly by vaccination, (4) inhibiting other effects of the disease, which may or may not be directly associated with amyloidosis (e.g., inflammation and oxidative

† We are grateful to the BBSRC (Grant number C14685 to A.J.D.), the AG Leventis Foundation (to N.K.), and the Wellcome Trust and BTG for funding Senexis.

* To whom correspondence should be addressed: Manchester Interdisciplinary Biocentre, The University of Manchester, 131 Princess Street, Manchester, M1 7DN, U.K. Telephone: +44-161-3064224. Fax: +44-161-2360409. E-mail: andrew.doig@manchester.ac.uk.

‡ The University of Manchester.

§ Senexis Limited.

[1] Abbreviations: AD, Alzheimer's disease; Aβ, β-amyloid; MTT, 3-(4,5-dimethylthiazol-2-yl)-2,5-diphenyltetrazolium bromide; ThT, thioflavin T; EM, electron microscopy; HFIP, hexafluoroisopropanol; TFA, trifluoroacetic acid.

10.1021/bi060837s CCC: $33.50
Published on Web 07/25/2006

stress), (5) replacing cells that have been killed by the disease (e.g., by cell or gene therapy), and (6) alleviating the symptoms of the disease but without necessarily blocking the pathogenic process.

The most effective treatments may be those designed to inhibit steps that *precede* protein/peptide aggregation, by blocking production of the amyloidogenic protein or peptide in the first place. However, this requires blocking the expression or activity of a natural protein or peptide that has presumably evolved to perform some other, important biological function in vivo. For example, many groups are currently developing inhibitors of β- or γ-secretase as potential drugs for AD. These two enzymes cleave amyloid precursor protein to produce the Aβ peptide associated with this disease, but they have also been shown to perform other, important biological functions (*10*). On the other hand, treatments designed to target steps that *follow* protein/peptide aggregation are less likely to be effective because they would not prevent the formation of toxic soluble oligomers or insoluble fibers, which could continue to kill cells. Thus, an attractive therapeutic strategy in principle is to inhibit protein/peptide aggregation itself, because this appears to be the first step in the pathogenic process of amyloidosis, which is not associated with some natural biological function (*11*, *12*).

An attractive strategy to develop amyloid aggregation inhibitors is to use the wild-type peptide, because it is already known to bind to itself, thus avoiding the usual necessity in drug discovery of finding a starting compound with some activity. The first group to make use of a core section of Aβ as a structural starting point was Tjernberg and co-workers, who showed that Aβ(16−20) was able to bind full-length Aβ and thus prevent its assembly into fibrils (*13*). Despite being shown to form fibrils in isolation, Aβ(16−20) (KLVFF) was proposed as being a key region from which a lead compound could be created against amyloid. Soto et al. also began work on inhibitors aimed at the core region of Aβ, in this case, residues 17−21 (LVFFA) (*14*). The strategy is based on substituting key residues for prolines in a bid to reduce the β propensity of the peptide, while retaining its hydrophobicity. A lead 11 amino acid inhibitor was reduced to five residues with greater ability to prevent fibril formation. All D analogues were found to be as effective but with increased protease resistance. These so-called β-sheet breaker peptides were shown not only to be stable in vivo but also to have blood−brain-barrier permeability (*15*, *16*). Initially on the the basis of the 15−25 region of Aβ, Murphy and workers designed a peptide with a "recognition element" homologous to the Aβ peptide but with a disrupting element of at least three lysines tagged to the C terminus, designed to interfere with Aβ aggregation (*17*−*19*). Sato et al. designed heptapeptide inhibitors of Aβ toxicity based on β-sheet packing (*20*). New types of small molecule inhibitors of Aβ aggregation have also recently been reported (*21*−*23*).

Here, we use N-methylated peptides (meptides) as inhibitors of amyloidosis. One side presents a hydrogen-bonding "complementary" face to the protein, with the other having *N*-methyl groups in place of backbone NH groups, thus presenting a "blocking" face. Substituents larger than a methyl group are also effective (*24*). We have previously shown that *N*-methyl derivatives of Aβ(25−35) are able to prevent aggregation and inhibit toxicity in PC12 cells (*25*). Meredith and co-workers (*26*, *27*) investigated N-methylated peptides of a region corresponding to 16−22 and later 16−20 of the amyloid "core domain" region. They can prevent Aβ fibrils from forming and break down preformed fibrils. These peptides have the added advantages of high proteolytic resistance, solubility, membrane permeability (*27*), and high propensity to form β structure at the N-methylated site. Cruz et al. found that single *N*-methyl amino-acid-containing peptides related to 16−20 of Aβ were able to reduce the cytotoxicity of Aβ(1−42) (*28*).

MATERIALS AND METHODS

Stock Preparation. Aβ(1−40) and Aβ(1−42) [(Cl) salt] was purchased from the American Peptide Company. A 10 mM stock solution of each target peptide in 1,1,1,3,3,3-hexafluoroisopropanol (HFIP) was prepared according to the Zagorski method to ensure that the peptide is initially in a monomeric state (*29*) as follows: (i) 3 cycles of dissolution with vortexing and sonication in high-grade trifluoroacetic acid (TFA, from Fluka) and drying under a slow stream of dry N_2, (ii) 3 cycles of dissolution (with vortexing and sonication) in high-grade HFIP and drying under a slow stream of dry N_2, (iii) dissolution of the target to 10 mM in HFIP, and (iv) storage of the 10 mM target stock solution in HFIP at 4 °C. TFA/HFIP treatment ensures that the amyloidogenic peptide is in a monomeric, soluble state.

Inhibitors (prepared by solid-phase Fmoc chemistry using *O*-(7-azabenzotriazol-1-yl)-1,1,3,3-tetramethyluronium as the coupling agent) were supplied in lyophilized form at >95% purity, verified by high-performance liquid chromatography (HPLC) and mass spectrometry, by Peptide Protein Research Ltd. (Southampton, U.K.). Inhibitors were dissolved to 1 mM (or in a few cases 0.5 or 2 mM) in 50% acetonitrile. In a few cases, some inhibitors were dissolved in 100% H_2O. The concentration of each Aβ-derived inhibitor was measured by its Phe absorbance at 257.4 nm ($\epsilon = 197\ M^{-1}\ cm^{-1}$ per Phe) or by weighing. The inhibitor solutions were stored at 4 °C prior to lyophilization of individual aliquots for each assay.

Thioflavin T (ThT). Inhibition assays were performed with 100 μM target peptide in 200 μL Dulbecco A phosphate-buffered saline (PBS) buffer (Oxoid), with or without each inhibitor at a concentration of 10 μM (for 1:0.1 molar ratio), 100 μM (for 1:1 molar ratio), or 1 mM (for 1:10 molar ratio). Sufficient target peptide was lyophilized, redissolved, and thoroughly vortexed as one single batch (for immediate use in all target−inhibitor mixes) to a concentration of 200 μM in pure, sterile-filtered ddH_2O to delay aggregation until the addition of each inhibitor. In parallel, 2 nmol (20 × 100 μL stock), 20 nmol (20 μL × 1 mM stock), or 200 nmol (200 μL × 1 mM stock) of each inhibitor was lyophilized and redissolved in a 1 mL Eppendorf tube to a concentration of 20 μM (1:0.1), 200 μM (1:1) or 2 mM (1:10), respectively, in 100 μL sterile-filtered 2× Dulbecco A PBS buffer (Oxoid: 320 mM NaCl, 6 mM KCl, 16 mM Na_2HPO_4, and 2 mM KH_2PO_4 at pH 7.4) All of the inhibitor solutions were then thoroughly vortexed to ensure complete dissolution. Finally, a 100 μL aliquot of the target solution was added to each 100 μL aliquot of inhibitor to give a total assay volume of 200 μL containing 100 μM target and either 10 μM, 100 μM, or 1 mM inhibitor in 1× Dulbecco PBS buffer. The

assay mixtures were vortexed and held in a 37 °C incubator for 4 days to induce aggregation in the presence of each inhibitor.

The ThT assay solution was prepared from stock containing 500 μM ThT in 50 mM glycine buffer at pH 8.5. The stock was aliquoted into 1 mL Eppendorfs and kept frozen until it was needed. It was then allowed to thaw at room temperature for 10 min before 25× dilution into the appropriate glycine buffer, giving the required freshly prepared ThT assay solution containing 20 μM ThT in 50 mM glycine buffer at pH 8.5. A total of 180 μL of the ThT assay solution was then added to each well of a 96-well black-bottomed microplate per desired repeat, using a multichannel pipet. Next, 20 μL aliquots of each inhibition/reversal assay mixture (thoroughly vortexed) were added to individual wells containing the ThT solution using an automated micropipet. The fluorescence of amyloid-bound ThT was measured in a Twinkle LB970 Fluorescence Plate Reader (Berthold Technologies) using the "top reading" setting with the lamp intensity set at 10 000 and a 3 s "shake" prior to each fluorescence reading, which was recorded over a period of 1 s using appropriate excitation and emission filters. Bound ThT excites at 450 nm and emits at 482 nm (*30*).

For the inhibition assays, the target−inhibitor mixtures were incubated at 37 °C. Single ThT readings were taken on days 1, 2, and 3, and five repeat readings were taken on day 4. For the reversal assays, the target was incubated alone at 37 °C for 3 days before the addition of 200 μL to each lyophilized inhibitor. The vortexed target−inhibitor solutions were then incubated at 37 °C for a further 4 days, during which time single ThT readings were taken on days 1, 2, and 3 and then five readings were taken on day 4 because maximal ThT binding was found after 4 days of aggregation (Figure A in the Supporting Information). A decrease in ThT fluoresence after 4 days may be due to the formation of larger fibrils that are able to bind a smaller amount of ThT. Inhibition/disaggregation activity was calculated by the percent reduction in the amyloid-bound ThT fluorescence of the target−inhibitor mixture compared with that of the target alone. The percentage amyloid is given by $(F_i - F_b)/(F_a - F_b) \times 100\%$, where the percentage of amyloid is the percent reduction in the amyloid-bound ThT fluorescence, F_i is the ThT fluorescence of the target−inhibitor mixture, F_a is the ThT fluorescence of the target alone, and F_b is the background ThT fluorescence with no target or inhibitor present.

Affinity Chromatography. Two copies of the Aβ core aggregation sequence were attached to the resin in tandem, linked by a pair of glycine residues for flexibility to allow for the formation of a β-turn/hairpin (sequence L-Ac-[(KLVFFAE)-GG]$_2$-resin). The affinity columns were synthesized by Peptide Protein Research Ltd. on a CP glass resin. The glass resin was chosen because of the inability of the inhibitor peptides to bind to the resin and for its incompressibility, allowing use in an HPLC system. All inhibitors were diluted to 100 μM stock solutions, containing 5% acetonitrile from their 1 mM stocks in 50% acetonitrile. A few inhibitor peptides were kept as 1 mM stocks in 100% H_2O and were diluted to 100 μM in 100% H_2O. A total of 180 μL of the 100 μM inhibitor stocks was transferred to specific inserts, which were then placed into vials. These specific HPLC vials were positioned on the autosampler of the Agilent Technologies HPLC instrument, where before the start of an affinity chromatography run, 50 μL would be collected from the insert and injected into the affinity column automatically, as controlled by the HPLC software (LC/MSD Chemstation, version A. 09.03). Each inhibitor was run through each affinity column 3 times using a linear gradient of 5−95% acetonitrile/0.1% TFA in ddH_2O/0.1% TFA for 33 min. The column was then washed with 95% acetonitrile/0.1% TFA for 2 min, decreased to 5% acetonitrile/0.1% TFA for 2 min, and equilibrated at 5% acetonitrile/0.1% TFA for 3 min, at a flow rate of 1 mL/min. The same cycle was repeated for each affinity run.

Electron Microscopy (EM). The same samples that were prepared for ThT fluorescence were also used for preparing samples for the EM assay. From the 200 μL that was prepared, 180 μL was used for the ThT assay and the remaining 20 μL was used for preparing EM samples. A total of 10 μL drops of the peptide solution samples were placed side by side on a clean strip of Parafilm along with 10 μL drops of 2% uranyl acetate (w/v in water) on another strip of Parafilm. Carbon-coated copper grids (400 mesh/inch) were then glow-discharged for 30 s to render them hydrophilic. The glow-discharged EM grids were then inverted on the peptide solution drops for 30 s, carefully blotted by touching the grid edge to the filter paper and negatively stained by inverting them on the uranyl acetated drop for 30 s. The grids were allowed to dry overnight. They were then ready for viewing under the microscope. Electron micrographs were recorded on a Philips EM 301 electron microscope at 100 kV at a magnification of 44000×.

3-(4,5-Dimethylthiazol-2-yl)-2,5-diphenyltetrazolium Bromide (MTT) Cell-Toxicity Assay. Rat phaeochromocytoma (PC12) cells were chosen for assessing toxicity because they have been identified as sensitive to the toxic effects of Aβ using MTT (*31*). The MTT cell titer 96 proliferation assay (Promega) is an in vitro assay measuring the conversion of the MTT tetrazolium component of the CellTitre 96 dye solution into a formazan product by the living PC12 cells, where the formazan product becomes solubilized and the absorbance is read at 570 nm. A color change takes place, and a measure of the percentage of MTT reduction is calculated, where the percentage of cellular MTT reduction provides an indication of the cell condition or health.

Briefly, 10 μM inhibitors were screened in the presence of 10 μM Aβ(1−42). The required volume from inhibitor and target stock solutions was freeze-dried overnight. The freeze-dried inhibitors and target peptide were resuspended in 100% dimethyl sulfoxide (DMSO), each at 2 mM concentration. A total of 5 μL from each of the resuspended inhibitor/DMSO and target/DMSO was mixed in a well of a 96-well preparation plate, thus giving 10 μL of 1:1 mM inhibitor/target concentration ratio in 100% DMSO. A total of 90 μL of Optimem media was added to the 10 μL inhibitor/target mixture (100:100 μM inhibitor/target ratio in 10% DMSO). A total of 10 μL of the 100:100 μM inhibitor/target mixture in 10% DMSO was then dispensed into 90 μL of media/PC12 cells ($n = 8$), at final inhibitor and target concentrations of 10 μM. These were incubated for 48 h at 37 °C, 5% CO_2, prior to the addition of the MTT dye. A total of 15 μL of the dye was added to each well and incubated for a further 4 h at 37 °C, 5% CO_2. A total of 100

μL of the stop/solubilization solution was then added to each well and was allowed to stand for 1 h. The absorbance was measured at 595 nm using a 96-well Tecan Ultra 384 plate reader. The percent MTT reduction was calculated as percent MTT reduction = $((x - A)/(B - A)) \times 100\%$, where x is the absorbance value in each well under study, A is the mean absorbance of the negative control, which corresponds to 0% MTT reduction because of the presence of dead cells (0.1% Triton X-100 with cells), and B is the positive control, which corresponds to 100% MTT reduction (live cells in 1% DMSO).

While the MTT assay with PC12 cells is the most widely used assay for measuring Aβ toxicity, we were concerned not to use this as the sole measure of toxicity. We therefore verified our MTT results with the SHSY5Y cell line and other indicators of cell viability, namely, calcein, lactate dehydrogenase, cell titer blue, and the tetrazolium salts XTT and MTS. We found that the MTT data were the most reproducible and required the lowest concentration of Aβ, giving a more useful concentration range for assaying inhibitors. The MTT results correlated well with all other methods (not shown), giving confidence in using MTT as our main toxicity assay.

RESULTS

Initial Library. The initial inhibitors were named SEN001−SEN021 (Table 1). These were mostly based around N-methylating the LVFF sequence, known to be key for amyloid formation in Aβ; in addition, KLVFF has been shown to act as an inhibitor of Aβ aggregation (*13*). Most were acetylated at the N terminus, and all were amidated at the C terminus, to more closely mimic the polypeptide backbone and provide additional potential hydrogen-bond acceptors and donors. Some peptides introduced specific amino acid substitutions to explore the effect of different residues on their ability to induce an inhibitory effect: peptides SEN001, SEN002, SEN011, SEN012, SEN014, SEN015, and SEN020 incorporated Lys at the N terminus, to include residue 16 of the Aβ wild-type sequence. SEN004−SEN010 had an additional glutamine at the N terminus, thus incorporating residue 15 of Aβ, and SEN020 included Glu at the C terminus, residue 22 of the wild-type sequence. SEN013 incorporated an Ala instead of Leu^{17}, while Lys^{16} changed positions with Phe^{19}, thus substituting a charged, hydrophilic side chain with an aromatic hydrophobic side chain at the N terminus. Reference peptides that had already been published as inhibitors of Aβ(1−40) and/or Aβ(1−42) amyloid formation were used as controls. These included SEN001 (*13*), SEN202 (*26*), PPI-1019 (*32*), and iAβ5p (*14*). D-iAβ5p was the enantiomer of iAβ5p, while C1 and C2 were control peptides anticipated to have no effect on Aβ.

The ThT results for inhibition of both Aβ(1−40) and Aβ-(1−42) for these peptides are shown in Figures A and B in the Supporting Information. Figure A in the Supporting Information shows that the inhibitors affect Aβ aggregation kinetics. The results for SEN001 and SEN002 confirm the results of Tjernberg et al. that nonmethylated KLVFF can act as an inhibitor. However, N-methylation reduced inhibitor activity for all of these L peptides. The most potent inhibitor in this round was the Praecis compound, PPI-1019, sequence D-[H-[(mL)-V-F-F-L]-NH_2], where methylation is on the N-terminal amine group, rather than a secondary amide in the backbone. We found no activity in iAβ5p, sequence L-[Ac-[L-P-F-F-D]-NH_2], previously reported as an Aβ aggregation inhibitor by Soto et al. (*14*). No activity was found for the control peptides, C1 and C2, as expected. These results were confirmed by EM, where Aβ fibril morphology was unchanged (data not shown). PPI-1019, the most potent inhibitor in the initial round, is a D amino acid peptide. ThT fluorescent studies by Chalifour et al. indicated that the D enantiomers of peptide-based inhibitors containing the KLVFF Aβ-recognition motif were more potent inhibitors of the natural L-Aβ(1−40)-induced aggregation and neurotoxicity than their natural L peptide counterparts (*33*). Similarly, the L peptides were more effective at inhibiting D-Aβ(1−40) aggregation than the D peptides. The results therefore indicate that these peptides can have an inhibitory effect of aggregation through a heterochiral type of stereospecificity. The inhibitors in the next round were therefore all D.

Round-1 Library. The round-1 library, sequences SEN101−SEN120 (Table 1), was based on the sequences of SEN018, SEN019, and PPI-1019. Specifically, the new library was composed of acetylated and corresponding nonacetylated peptides, all composed of the LVFFL domain, that were singly, doubly, or triply methylated. The peptides were all D enantiomers and were amidated at the C terminus. The aim of the round-1 library was to assess the effect of acetylation or nonacetylation and to identify the best sites for N-methylation. All inhibitors were assayed by binding affinity, ThT, and EM and compared to C1, C2, SEN018, SEN019, PPI-1019, and iAβ5p. The rest of the library was derived from SEN019 and composed of the LVFFL hydrophobic domain, incorporating either single, double, or triple methylations. Results are shown in Figures 1−3.

As shown in Figure Aa in the Supporting Information, the range of activities of the round-1 inhibitors on Aβ(1−40) is from 10 to 100% when assayed with ThT, with errors of typically 15%, showing that reliable ranking of inhibitors was possible. The best round-1 inhibitors reduce amyloid formation by Aβ(1−40) to 24, 23, and 13% for SEN101, SEN113, and SEN116, respectively (compared with 64−70 and 44−80% for SEN018 and SEN019, respectively, and 35−42% for PPI-1019). SEN113 and SEN116 are more active against Aβ(1−40) than PPI-1019, as well as iAβ5p, which had 61% amyloid formation. SEN101 is an acetylated peptide, singly N-methylated at the N-terminal Leu residue (X1), while SEN113 is nonacetylated, singly N-methylated at the C-terminal Leu (X5). SEN116, the best inhibitor studied to this point, is also nonacetylated but double-methylated at both the N- and C-terminal leucines (X1 and X5). Other peptides, including SEN105 and SEN117, had no effect.

Structure/activity relationships could be inferred by comparing inhibitors differing by a single substituent: the acetylated inhibitors were generally less potent than their nonacetylated counterparts; methylation of the X3 position causes a very negative inhibitory effect, especially when X1 and/or X5 are/is also methylated; methylation of X1 and/or X5 is very favorable; methylation of X2 and/or X4 are/is better than methylation of X3 but not as good as methylation of X1 and/or X5. Overall, the best inhibitor is SEN116,

Table 1: Inhibitor Sequences[a]

name	chirality	sequence	name	chirality	sequence
SEN001	L	Ac-[K-L-V-F-F-A]-NH_2	SEN230	D	H-[(mL)-(chGly)-F-F-(mL)]-NH_2
SEN002	L	Ac-[K-L-V-F-F]-NH_2	SEN231	D	H-[(mL)-(chAla)-F-F-(mL)]-NH_2
SEN003	L	Ac-[L-V-F-F-A]-NH_2	SEN232	D	H-[(mL)-(hPhe)-F-F-(mL)]-NH_2
SEN004	L	Ac-[Q-K-L-V-F-F]-NH_2	SEN233	D	H-[(mL)-(2nAla)-F-F-(mL)]-NH_2
SEN005	L	Ac-[Q-K-(mL)-V-F-F]-NH_2	SEN241	D	H-[(mL)-V-A-F-(mL)]-NH_2
SEN006	L	Ac-[Q-K-L-(mV)-F-F]-NH_2	SEN242	D	H-[(mL)-V-V-F-(mL)]-NH_2
SEN007	L	Ac-[Q--K-L-V-(mF)-F]-NH_2	SEN243	D	H-[(mL)-V-I-F-(mL)]-NH_2
SEN008	L	Ac-[Q-K-L-V-F-(mF)]-NH_2	SEN244	D	H-[(mL)-V-L-F-(mL)]-NH_2
SEN009	L	Ac-[Q-K-(mL)-V-(mF)-F]-NH_2	SEN245	D	H-[(mL)-V-M-F-(mL)]-NH_2
SEN010	L	Ac-[Q-K-L-(mV)-F-(mF)]-NH_2	SEN116	D	H-[(mL)-V-F-F-(mL)]-NH_2
SEN011	L	Ac-[K-L-(mV)-F-(mF)-A]-NH_2	SEN247	D	H-[(mL)-V-Y-F-(mL)]-NH_2
SEN012	L	Ac-[K-(mL)-V-(mF)-F-(mA)]-NH_2	SEN248	D	H-[(mL)-V-W-F-(mL)]-NH_2
SEN013	L	Ac-[F-A-(mF)-K-(mV)-L]-NH_2	SEN249	D	H-[(mL)-V-(tbGly)-F-(mL)]-NH_2
SEN014	L	Ac-[K-L-(mV)-F-(mF)]-NH_2	SEN250	D	H-[(mL)-V-(chGly)-F-(mL)]-NH_2
SEN015	L	Ac-[K-(mL)-V-(mF)-F]-NH_2	SEN251	D	H-[(mL)-V-(chAla)-F-(mL)]-NH_2
SEN016	L	Ac-[L-(mV)-F-(mF)-A]-NH_2	SEN252	D	H-[(mL)-V-(hPhe)-F-(mL)]-NH_2
SEN017	L	Ac-[(mL)-V-(mF)-F-(mA)]-NH_2	SEN253	D	H-[(mL)-V-(2nAla)-F-(mL)]-NH_2
SEN018	D	Ac-[L-(mV)-F-(mF)-L]-NH_2	SEN261	D	H-[(mL)-V-F-A-(mL)]-NH_2
SEN019	D	Ac-[(mL)-V-(mF)-F-(mL)]-NH_2	SEN262	D	H-[(mL)-V-F-V-(mL)]-NH_2
SEN020	L	Ac-[K-(mL)-V-(mF)-F-(mA)-E]-NH_2[b]	SEN263	D	H-[(mL)-V-F-I-(mL)]-NH_2
SEN021	L	Ac-[P-L-V-F-F-A]-NH_2	SEN264	D	H-[(mL)-V-F-L-(mL)]-NH_2
PPI-1019	D	H-[(mL)-V-F-F-L]-NH_2[c]	SEN265	D	H-[(mL)-V-F-M-(mL)]-NH_2
SEN025	L	Ac-[L-P-F-F-A]-NH_2	SEN116	D	H-[(mL)-V-F-F-(mL)]-NH_2
iAβ5p	L	Ac-[L-P-F-F-D]-NH_2[d]	SEN267	D	H-[(mL)-V-F-Y-(mL)]-NH_2
D-iAβ5p	D	Ac-[L-P-F-F-D]-NH_2	SEN268	D	H-[(mL)-V-F-W-(mL)]-NH_2
C1	L	Ac-[S-K-S-G-Y]-NH_2	SEN269	D	H-[(mL)-V-F-(tbGly)-(mL)]-NH_2
C2	L	Ac-[Y-G-S-K-S]-NH_2	SEN270	D	H-[(mL)-V-F-(chGly)-(mL)]-NH_2
SEN101	D	Ac-[(mL)-V-F-F-L]-NH_2	SEN271	D	H-[(mL)-V-F-(chAla)-(mL)]-NH_2
SEN102	D	Ac-[L-V-(mF)-F-L]-NH_2	SEN272	D	H-[(mL)-V-F-(hPhe)-(mL)]-NH_2
SEN103	D	Ac-[L-V-F-F-(mL)]-NH_2	SEN273	D	H-[(mL)-V-F-(2nAla)-(mL)]-NH_2
SEN104	D	Ac-[(mL)-V-(mF)-F-L]-NH_2	SEN280	D	H-[(mL)-V-F-F-(none)]-NH_2
SEN105	D	Ac-[L-V-(mF)-F-(mL)]-NH_2	SEN281	D	H-[(mL)-V-F-F-A]-NH_2
SEN106	D	Ac-[(mL)-V-F-F-(mL)]-NH_2	SEN282	D	H-[(mL)-V-F-F-V]-NH_2
SEN019	D	Ac-[(mL)-V-(mF)-F-(mL)]-NH_2	SEN283	D	H-[(mL)-V-F-F-I]-NH_2
SEN108	D	Ac-[L-(mV)-F-F-L]-NH_2	PPI-1019	D	H-[(mL)-V-F-F-L]-NH_2[c]
SEN109	D	Ac-[L-V-F-(mF)-L]-NH_2	SEN285	D	H-[(mL)-V-F-F-M]-NH_2
SEN018	D	Ac-[L-(mV)-F-(mF)-L]-NH_2	SEN289	D	H-[(mL)-V-F-F-(tbGly)]-NH_2
PPI-1019	D	H-[(mL)-V-F-F-L]-NH_2[c]	SEN290	D	H-[(mL)-V-F-F-(chGly)]-NH_2
SEN112	D	H-[L-V-(mF)-F-L]-NH_2	SEN291	D	H-[(mL)-V-F-F-(chAla)]-NH_2
SEN113	D	H-[L-V-F-F-(mL)]-NH_2	SEN292	D	H-[(mL)-V-F-F-(hPhe)]-NH_2
SEN114	D	H-[(mL)-V-(mF)-F-L]-NH_2	SEN293	D	H-[(mL)-V-F-F-(2nAla)]-NH_2
SEN115	D	H-[L-V-(mF)-F-(mL)]-NH_2	SEN301	D	H-[(chGly)-(chAla)-(chGly)-(chGly)-(mL)]-NH_2
SEN116	D	H-[(mL)-V-F-F-(mL)]-NH_2	SEN302	D	H-[(chAla)-(chGly)-(chGly)-(mL)]-NH_2
SEN117	D	H-[(mL)-V-(mF)-F-(mL)]-NH_2	SEN303	D	H-[(chAla)-(chAla)-(chGly)-(chGly)-(mL)]-NH_2
SEN118	D	H-[L-(mV)-F-F-L]-NH_2	SEN304	D	H-[(chGly)-(Y)-(chGly)-(chGly)-(mL)]-NH_2
SEN119	D	H-[L-V-F-(mF)-L]-NH_2	SEN305	D	H-[(chGly)-(chAla)-(tbuGly)-(chGly)-(mL)]-NH_2
SEN120	D	H-[L-(mV)-F-(mF)-L]-NH_2	SEN306	D	H-[(chGly)-(chAla)-(chAla)-(chGly)-(mL)]-NH_2
SEN200	D	H-[(none)-V-F-F-(mL)]-NH_2	SEN307	D	H-[(chGly)-(chAla)-(chGly)-(chGly)-(mA)]-NH_2
SEN201	D	H-[A-V-F-F-(mL)]-NH_2	SEN313	D	Ac-[V-I-L-(mL)]-NH_2
SEN202	D	H-[V-V-F-F-(mL)]-NH_2	SEN314	D	H-[V-I-L-(mL)]-NH_2
SEN203	D	H-[I-V-F-F-(mL)]-NH_2	SEN315	D	Ac-[K-V-I-L-(mL)]-NH_2
SEN113	D	H-[L-V-F-F-(mL)]-NH_2	SEN316	D	H-[K-V-I-L-(mL)]-NH_2
SEN205	D	H-[M-V-F-F-(mL)]-NH_2	SEN317	D	Ac-[I-V-I-L-(mL)]-NH_2
SEN206	D	H-[F-V-F-F-(mL)]-NH_2	SEN318	D	H-[I-V-I-L-(mL)]-NH_2
SEN207	D	H-[Y-V-F-F-(mL)]-NH_2	SEN319	D	H-[I-V-L-L-(mL)]-NH_2
SEN208	D	H-[W-V-F-F-(mL)]-NH_2	SEN320	D	H-[I-V-L-I-(mL)]-NH_2
SEN209	D	H-[(tbGly)-V-F-F-(mL)]-NH_2	SEN321	D	H-[I-V-I-I-(mL)]-NH_2
SEN210	D	H-[(chGly)-V-F-F-(mL)]-NH_2	SEN322	D	H-[I-V-I-L-(mA)]-NH_2
SEN211	D	H-[(chAla)-V-F-F-(mL)]-NH_2	SEN401	D	H-[(chGly)-Y-(chGly)-(chGly)-L]-NH_2
SEN212	D	H-[(hPhe)-V-F-F-(mL)]-NH_2	SEN402	D	H-[Y-(chGly)-(chGly)-L]-NH_2
SEN213	D	H-[(2nAla)-V-F-F-(mL)]-NH_2	SEN403	D	H-[(chGly)-Y-(chGly)-(chGly)-(chGly)]-NH_2
SEN221	D	H-[(mL)-A-F-F-(mL)]-NH_2	SEN404	D	H-[Y-(chGly)-(chGly)-(chGly)]-NH_2
SEN116	D	H-[(mL)-V-F-F-(mL)]-NH_2	SEN405	D	H-[(chGly)-(chGly)-(chGly)-(chGly)-(chGly)]-NH_2
SEN223	D	H-[(mL)-I-F-F-(mL)]-NH_2	SEN406	D	H-[(chGly)-(chGly)-(chGly)-(chGly)]-NH_2
SEN224	D	H-[(mL)-L-F-F-(mL)]-NH_2	SEN407	D	H-[I-V-I-L-L]-NH_2
SEN225	D	H-[(mL)-M-F-F-(mL)]-NH_2	SEN408	D	H-[V-I-L-L]-NH_2
SEN226	D	H-[(mL)-F-F-F-(mL)]-NH_2	SEN409	D	H-[I-V-I-I-I]-NH_2
SEN227	D	H-[(mL)-Y-F-F-(mL)]-NH_2	SEN410	D	H-[V-I-I-I]-NH_2
SEN228	D	H-[(mL)-W-F-F-(mL)]-NH_2	SEN411	D	H-[(chGly)-(chGly)-(chGly)]-NH_2
SEN229	D	H-[(mL)-(tbGly)-F-F-(mL)]-NH_2			

[a] Abbrevations: *tert*-butyl-Gly (tbGly), cyclohexyl-Gly (chGly), cyclohexyl-Ala (chAla), homo-Phe (hPhe), and 2-naphthyl-Ala (2nAla). [b] From ref *26*. [c] From ref *32*. [d] From ref *14*.

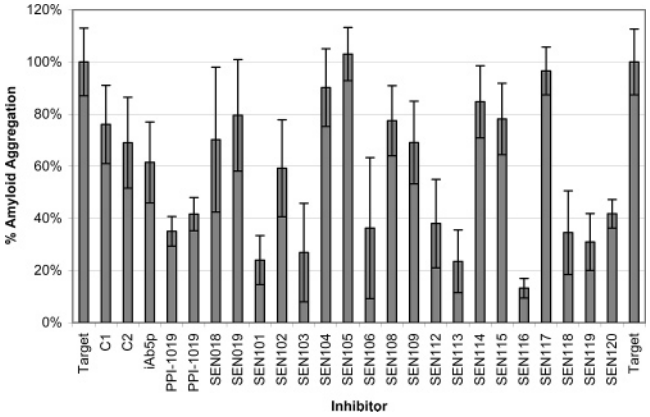

FIGURE 1: Round-1 ThT assay. Aβ(1−40), 100 μM; inhibitor, 100 μM. Error = 1 standard deviation; $n = 3$. Aβ(1−40) (100 μM) in isolation is scaled to 100%.

which fits with these conclusions, being nonacetylated and having methylated residues at the X1 and X5 positions.

A selection of the best inhibitors were then tested against Aβ(1−42) to determine their effect on this more amyloidogenic peptide (Figure C in the Supporting Information). Amyloid formation was reduced to 52, 51−70, and 62% for SEN101, PPI-1019, and SEN116, respectively. These were smaller reductions than with Aβ(1−40), confirming that the longer peptide is a more challenging target. Interestingly, iAβ5p induces Aβ(1−42) aggregation, shown by the higher ThT fluorescence than that of the target alone. Overall, SEN101 and PPI-1019, both methylated at the N-terminal Leu, as well as SEN116, methylated at both the N- and C-terminal leucines, are the best modulators of Aβ(1−42) aggregation. In contrast to Aβ(1−40), SEN113, methylated only at the C-terminal Leu of the LVFFL domain, did not have high inhibitor activity, suggesting that, when methylating at the fifth (X5) position, inhibition is decreased. Structure/activity relationships indicated that acetylated inhibitors were less potent than their nonacetylated counterparts, methylation at the first (X1) position was only favored when X5 was methylated (as in SEN113 and SEN116). Overall, only methylation of X1 is undoubtedly favorable.

Selected round-1 inhibitors were assayed for their ability to reverse aggregation by Aβ(1−40) and Aβ(1−42) (Figure D in the Supporting Information). Each target was allowed to aggregate for 3 days at 37 °C prior to the addition of 100 μM of each inhibitor for a subsequent period of 4 days. C1, C2, and iAβ5p could not reverse aggregation of Aβ(1−40), while all of the all-D-peptide inhibitors tested gave about 20−40% reversal (as opposed to 60−80% inhibition at the same inhibitor/target concentrations). PPI-1019 had the highest potency in reversing Aβ(1−40) fibril formation by reducing aggregation to 59%. SEN101, SEN113, and SEN116 were able to reverse Aβ(1−40) aggregation to 65−71%. Only PPI-1019 was able to reverse Aβ(1−42) aggregation.

The round-1 inhibitors were all tested 3 times on the Aβ-affinity column, giving highly reproducible results with a standard deviation of less than 0.2 min. Peptides that were found to bind tightly to the columns did not bind to the CPG glass resin, confirming that the inhibitors do not bind to any other component of the system besides the target peptide attached to the resin. Results are shown in Figure 2. The acetylated peptides bind to the column more tightly than the

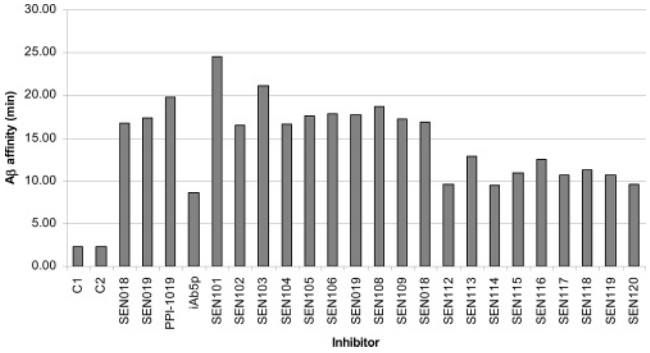

FIGURE 2: Round-1 affinity chromatography.

nonacetylated peptides. Within each acetylated or nonacetylated series, however, structure/activity relationships could be inferred that agree well with ThT results. The control peptides, C1 and C2, did not bind at all. iAβ5p bound poorly to the Aβ column, in agreement with ThT results. All of the methylated inhibitors bound to the columns, indicating that methylation increases the binding affinity of the peptides, unlike proline (as in iAβ5p). Specifically, PPI-1019, being methylated at the X1 position only, reported strong binding affinity, thus suggesting that the first residue should be methylated in Aβ inhibitors. Moreover, SEN113 and SEN116, methylated at X5 and X1/X5, respectively, were tightly bound peptides, correlating with ThT activity, which suggested that methylation of X1 and/or X5 is favorable. These results suggested that the affinity chromatography method could give valuable results, provided that all of the inhibitors are N-methylated and unacetylated, so that they are soluble and do not aggregate.

EM was performed on selected round-1 inhibitors to assess fibril morphology of Aβ(1−40) and Aβ(1−42) in the presence or absence of inhibitors (Figure 3 and Table 2). Samples were prepared from the same sample used for ThT fluorescence spectroscopy to directly compare results. Aβ-(1−40) is characterized by large fibril networks, composed of long, single, straight, unbranched fibers of varying length and 9−14 nm in diameter. The fibril diameter in the presence of PPI-1019 and SEN113 increases to 14−17 and 8−20 nm, respectively, while remaining unaltered in the presence of SEN116. There is a reduction in the number and length of fibers present with PPI-1019, SEN113, and SEN116. The most obvious morphological change took place in the presence of SEN116, where the fibril length was considerably reduced to 200−500 nm. SEN116 caused changes in fibril association, where two fibrils were laterally associated; a few twisted ribbons were also present with a helical repeat of 100−200 nm. Aβ(1−42) formed a similar morphology to Aβ(1−40), although the fibril diameter was slightly larger, forming long twisted ribbons with no apparent lateral association. PPI-1019 and SEN116 caused a reduction in fibril formation as well as altering fibril length in Aβ(1−42), supporting the ThT results.

Round-2 Library. The round-1 results suggested the following preferred features for an Aβ aggregation inhibitor: derivatives of LVFFL, all D peptide enantiomers, nonacetylated, C-terminally amidated, and single methylations at residues of the first or fifth positions or double methylations at both the first and fifth positions.

To identify the optimal side chain at each position, 13 different residues were substituted at each position in turn,

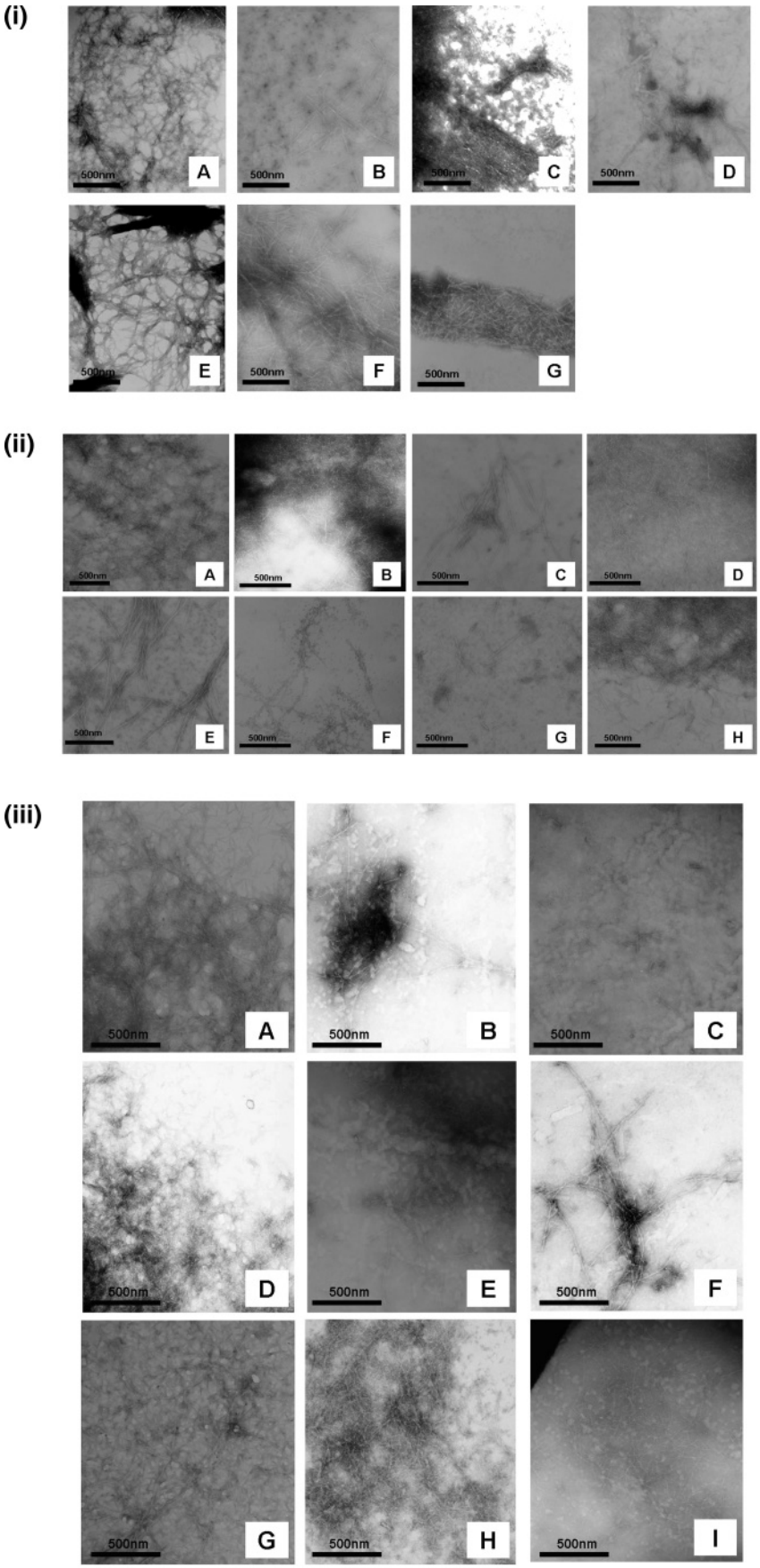

FIGURE 3: Electron micrographs. All at 0.1:1 inhibitor/target ratio (10 μM inhibitor/100 μM target). (i) (A) Aβ(1−40), (B) Aβ(1−40)/PPI-1019, (C) Aβ(1−40)/SEN113, (D) Aβ(1−40)/SEN116, (E) Aβ(1−42), (F) Aβ(1−42)/PPI-1019, and (G) Aβ(1−42)/SEN116. (ii) (A) Aβ(1−40)/C2, (B) Aβ(1−40)/SEN200, (C) Aβ(1−40)/SEN211, (D) Aβ(1−40)/SEN221, (E) Aβ(1−40)/SEN231, (F) Aβ(1−40)/SEN250, (G) Aβ(1−40)/SEN270, and (H) Aβ(1−40)/SEN281. (iii) Aβ(1−40) in the presence of (A) SEN301, (B) SEN 303, (C) SEN304, (D) SEN313, (E) SEN318, (F) SEN319, (G) SEN321, and (H) SEN323.

Table 2: Fibril Morphology of Aβ(1−40) and Aβ(1−42) in the Presence of Selected Inhibitors as Detected by EM

target (100 μM)	inhibitor name	inhibitor concentration (μM)	diameter (nm)	length (nm)	fibril morphology
Aβ(1−40)	N/A	N/A	9−14	N/A	long, single fibers without obvious twists or lateral association
Aβ(1−42)	N/A	N/A	10−17	N/A	long twisted ribbons, no apparent lateral association
Aβ(1−40)	PPI-1019	100	14−17	600−700	lateral fibril association composed of two fibers, few twisted ribbons with helical repeat of 100−200 Å
Aβ(1−40)	SEN113	100	8−20	500−700	straight unbranched fibers
Aβ(1−40)	SEN116	100	7−15	200−500	lateral fibril association composed of two fibers, single narrower fibers also present, no twisted ribbons
Aβ(1−42)	PPI-1019	100	10−14	300−600	twisted ribbons and single fibers present, no apparent lateral association
Aβ(1−42)	SEN116	100	10−13	100−250	unable to distinguish lateral or twisted fibril morphology
Aβ(1−40)	C2	10	8−11	N/A	long, single fibers without obvious twists or lateral association, similar to target alone
Aβ(1−40)	SEN200	10	11−18	N/A	long, single fibers without obvious twists or lateral association, similar to target alone
Aβ(1−40)	SEN211	10	15−19	300−1150	twisted ribbons usually composed of two−three fibers and few fibers arranged by lateral association
Aβ(1−40)	SEN221	10	8−12	N/A	long, single fibers without obvious twists or lateral association, similar to target alone
Aβ(1−40)	SEN231	10	12−24	500−950	short, unbranched twisted ribbons composed of two fibers, few fibers associating laterally, less fibril networks than the wild type
Aβ(1−40)	SEN250	10	6−8	800−1200	few but very long, straight twisted ribbons composed of two fibers no lateral association
Aβ(1−40)	SEN270	10	14−19	200−300, 600−800	small networks of fibers present, few twisted ribbons composed of two fibers and few single fibers arranged laterally
Aβ(1−40)	SEN281	10	12−17	100−600	single twisted fibers forming large networks similar to the wild type, few straight short fibers present
Aβ(1−40)	SEN301	10	8−16	180−190, 600−700, 1500−1600	long, single fibers and twisted ribbons composed of two or more fibers, more than one fibril population present
Aβ(1−40)	SEN303	10	11−18	400−500, 800−1200, 1600−1700	long, single fibers with bends and twisted ribbons composed of two fibers
Aβ(1−40)	SEN304	10	13−23	200−300	twisted ribbons usually composed of two fibers with helical repeat of 100 nm, few single fibers, grid full of isolated small fibers
Aβ(1−40)	SEN313	10	10−20	N/A	long, single fibers without obvious twists or lateral association, similar to target alone
Aβ(1−40)	SEN318	10	12−21	900−1100	very long twisted ribbons composed of two fibers, some too long to measure, large fibril networks present
Aβ(1−40)	SEN319	10	18−22	1200−1800	twisted ribbons composed of more than two fibers with helical repeat of 120 nm
Aβ(1−40)	SEN321	10	10−22	1800−1900	very long twisted ribbons composed of two fibers with helical repeat of 350 nm, few clusters of fibers present
Aβ(1−40)	SEN323	10	10−16	N/A	long, single fibers without obvious twists or lateral association, similar to target alone, few large fibril networks present

while taking the remaining four positions from H-[(mL)-V-F-F-(mL)]-NH_2 (SEN116). The side chains tested were A, V, I, L, M, F, Y, W, *tert*-butyl-Gly (tbGly), cyclohexyl-Gly (chGly), cyclohexyl-Ala (chAla), homo-Phe (hPhe), and 2-naphthyl-Ala (2nAla). Uncharged and nonpolar side chains were chosen because the target region of Aβ is assumed to also be nonpolar. Nonnatural amino acids were included to test many potentially interesting derivatives. The N- and C-terminal residues were also deleted. The entire round-2 library is listed in Table 1 and named SEN200−SEN293, where SEN200−SEN213 are modified at position 1, SEN221−SEN233 are modified at position 2, SEN241−SEN253 are modified at position 3, SEN261−SEN273 are modified at position 4, and SEN270−SEN283 are modified at position 2. The side chains are numbered in the same order within each of the five series; e.g., SEN205, SEN225, SEN245, SEN265, and SEN285 have Met at positions 1−5, respectively. Peptides that had been previously used retained their former names. The control peptides, C1 and C2, iAβ5p, and the three best peptide inhibitors identified in round 1, namely, PPI-1019, SEN113, and SEN116, were also included.

With the improved activity of the inhibitors, the inhibitor/Aβ stoichiometry was reduced to 0.1:1 (10 μM inhibitor/100 μM Aβ) to maximize the range of results. The best round-2 inhibitors now reduced amyloid formation by Aβ-(1−40) to 50% (Figure 4), showing the best side chains at each position to be (1) (chGly/2nAla/chAla) > (hPhe/Trp/Leu) > (Val/Ile/Phe); (2) (chAla/Tyr) > (chGly/Phe/Trp/Leu/2nAla) > (Val/Ile); (3) (chGly/chAla/tbGly) > (2nAla/Leu/hPhe/Trp) > (Ile/Phe); (4) (chGly/2nAla/Ile) > (chAla/Leu/tbGly) > (Val/Met); and (5) (Ala/Val) > (tbGly/Met).

All round-2 peptides were tested 3 times on Aβ-affinity columns, giving data that support the ThT results (Figure 5). In general, the binding affinity of the SEN200−SEN293 peptide libraries increased with the hydrophobicity of the alternative substituted residue, although some smaller and less hydrophobic side chains did increase the binding affinity in certain positions, such as Val at position 2 (SEN222) and Ile at the second, third, and fourth positions (SEN223,

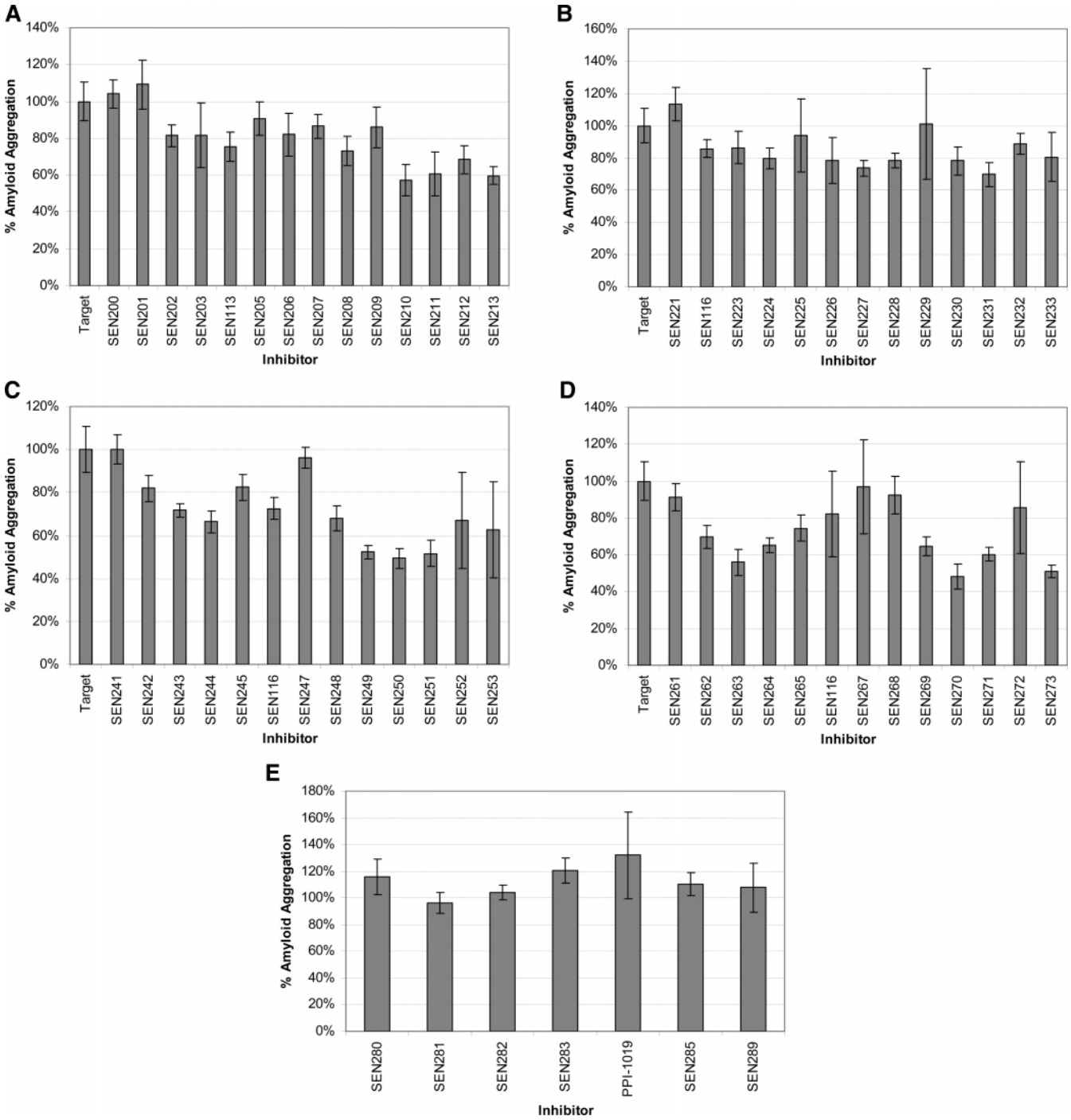

FIGURE 4: Round-2 ThT assay. Aβ(1−40), 100 μM; inhibitor, 10 μM. Error = 1 standard deviation; n = 3. Aβ(1−40) (100 μM) in isolation is scaled to 100%.

SEN243, and SEN263, respectively). These results therefore provided an opportunity to design peptides with increased binding affinity while reducing the molecular weight. It should also be noted that the SEN280−SEN293 library, where the last residue is unmethylated, bound very tightly to the affinity column. This could be due to the aggregation of the inhibitors on the affinity column because of nonmethylation of the last residue. Figure E in the Supporting Information shows good correlations between affinity binding and ThT results for each of the SEN200−SEN273 series but no correlation for the SEN280−SEN293 series.

Electron micrographs showing Aβ(1−40) in the presence of selected round-2 inhibitors are shown in Figure 3 and summarized in Table 2. SEN211, SEN231, SEN250, SEN270, and SEN281 were chosen to study because they were identified as among the most active inhibitors against Aβ-(1−40) aggregation by ThT. SEN201 and SEN221 were chosen because of their inability to inhibit amyloid formation by Aβ(1−40). C2, SEN200, and SEN221 had no effect on fibril formation. In the presence of the active selected round-2 inhibitors, a clear change in fibril morphology was detected with a reduction in the fibril length, while the number of large fibril networks throughout the EM grid was considerably reduced. In general, the fibril diameter ranged from 12 to 18 nm, although there were cases where the fibril diameter was either increased or reduced, depending upon the inhibitor

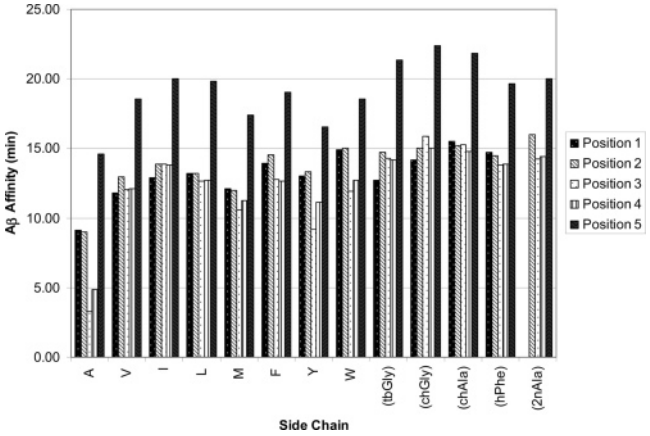

FIGURE 5: Round-2 affinity chromatography.

effect. For example, SEN250 caused the most obvious morphology change, where the fibril diameter was reduced to 6−8 nm, while the fibril length was relatively longer than other inhibitor effects (up to 1200 nm). SEN231, however, which was also found to have a similar inhibitory effect to SEN250 against Aβ(1−40) (by ThT), caused a different morphology change: the fibril diameter was thicker than Aβ-(1−40) alone, reaching 24 nm in diameter, while the fibril length was reduced to 500−950 nm. Moreover, inhibitors appeared to induce fibril association, where a small number of twisted ribbons were formed (as opposed to single, long fibers forming complex fibril networks by the amyloidogenic target), usually composed of two−three fibers with a helical repeat of 200 nm.

Round-3 Library. A total of 18 new inhibitors, combining the best side chains, were designed, synthesized, and studied (SEN301−SEN324; Table 1). All peptides were based on combinations of the best side chains at each position, with one or two alternative side chains substituted at each position. Larger aromatic side chains (Trp and 2nAla) were avoided, where possible, to maintain a lower molecular weight and avoid potential oxidation in vivo. N-Terminal truncations of combined sequences were also included to determine whether the weight can be reduced without the loss of activity. The round-3 peptide inhibitors were compared directly to the standard control peptides, namely, C1, C2, PPI-1019, and iAβ5p, as well as the best compounds from round 1 (PPI-1019, SEN113, and SEN116) and the most active inhibitors from round 2 (SEN211, SEN231, SEN250, SEN271, SEN208, and SEN228).

ThT results are shown in Figure 6. The inhibitor/Aβ stoichiometry was again 0.1:1 [10 μM inhibitor/100 μM Aβ-(1−40)]. SEN304 D-(H-[(chGly)-(Tyr)-(chGly)-(chGly)-(mLeu)]-NH_2) was the most active compound, being able to inhibit Aβ(1−40) aggregation to 43%. Figure 7 shows Aβ-affinity chromatography results. SEN301 had the strongest binding affinity to the Aβ column. SEN302, SEN305, and SEN306 also bound tightly to the Aβ column. SEN304 bound relatively tightly to the Aβ column, although not as tightly as SEN301. When the N-terminal residue was missing or polar, as in SEN314, SEN315, and SEN316, there was no binding. The correlation between the ThT and affinity results was weak within this library.

Figure 3 presents the fibril morphology of a selection of the most active round-3 inhibitors in the presence of Aβ-(1−40), namely, SEN303, SEN304, SEN318, SEN319, and

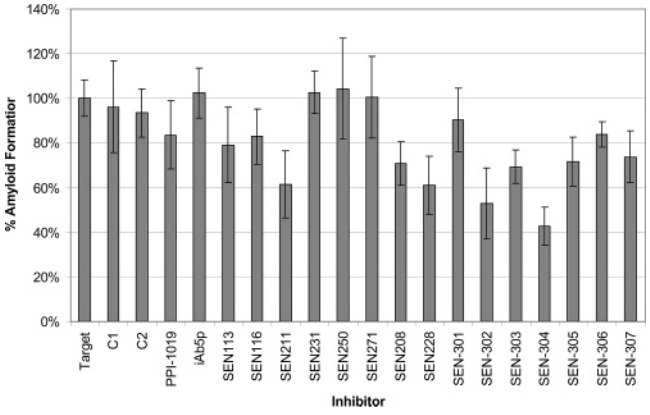

FIGURE 6: Round-3 ThT assay. Aβ(1−42), 10 μM; inhibitor, 5 μM. Error = 1 standard deviation; n = 3. Aβ(1−42) (10 μM) in isolation is scaled to 100%.

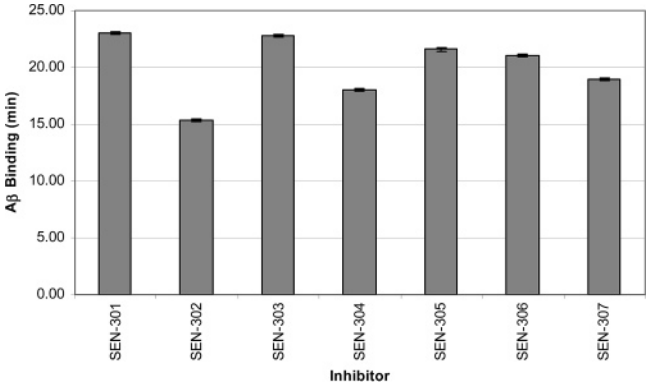

FIGURE 7: Round-3 affinity chromatography.

SEN321, as well as three of the least active inhibitor peptides against Aβ(1−40) aggregation, which include SEN301, SEN313, and SEN323. Fibers formed by inhibitor/target mixtures were of varying length and morphology. Specifically, the peptides that had been identified as poor inhibitors of amyloid formation by Aβ(1−40) (SEN301, SEN313, and SEN323), all exhibited a similar morphology, which was closely related to the target alone. They were characterized by the formation of large fibril networks throughout the EM grid, composed of very long single fibers with a relatively small diameter of 8−16 nm. SEN301/Aβ(1−40) also formed more than one fibril population in terms of length, ranging from 180 to 1600 nm. A selection of the best inhibitors of Aβ(1−40) fibrillogenesis, which included SEN303, SEN318, SEN319, and SEN321, were characterized by the formation of thicker fibers with the average diameter ranging from 10 to 22 nm and the formation of straight but twisted ribbons usually composed of two−three fibers with a helical repeat of 100−120 or even 350 nm (as was the case with SEN319 and SEN321). It was evident, however, that the presence of the inhibitors not only changed the morphology of the fibers but also reduced the abundance of fibrils in solution, and consequently, only a few and small clustered fibril aggregates could be identified. The effect of the good inhibitors on fibril length varied. For example, SEN303 exhibited more than one fibril length, while SEN318, SEN319, and SEN321 formed long fibers that were shorter than the Aβ alone (because they could be measured) but were still longer than the average length of fibril formation in inhibitor/target mixtures. The most striking evidence of inhibitor activity

against Aβ(1−40) aggregation was the effect of SEN304. SEN304/Aβ(1−40) formed very short (200−300 nm) twisted ribbons composed of two fibers with a helical repeat of 100 nm and a diameter length of 13−23 nm. The most obvious effect on inhibition was the absence of large fibril networks or any formation of clustered aggregates (as detected by all of the previously mentioned mixtures). Instead, it was characterized by small isolated fibers that were present throughout the EM grid (and thus throughout the solution) that could only be detected at high magnification. These isolated fibers may have contributed to the 40% amyloid formation observed by ThT. These results support the ThT assay, which indicated that SEN304 was the most potent inhibitor of Aβ(1−40) aggregation.

Round-4 Library. The round-4 peptides (SEN401−SEN411) were all nonmethylated, to test the hypothesis that N-methylation is useful for inhibitor activity. SEN401 is nonmethylated SEN304. SEN402−SEN406 and SEN411 contained multiple chGly residues to test whether the activity in the best round-3 inhibitors was a nonspecific property of this side chain. SEN407−SEN410 were nonmethylated derivatives of promising compounds from round 3 that were based on Val, Ile, and Leu side chains.

All of the round-4 peptides proved to be very difficult to work with, because of the low solubility in aqueous solvents, precluding the collection of ThT data. Because it was often not possible to achieve an adequate concentration of peptide, it was difficult to assess their efficacy. In the affinity assay, SEN402 eluted at 17.49 min, while SEN404 did not bind at all; affinity data on the other round-4 peptides could not be acquired.

MTT Toxicity Assay. Figure 8 shows results from the MTT toxicity assay using Aβ(1−42) and selected inhibitors. The assay was performed with 10 μM Aβ(1−42) and 10 μM inhibitor (Figure 8A) or 5 μM inhibitor (Figure 8B). The MTT reduction with MTT alone was 25−30%. None of the inhibitors studied here increased toxicity, while many partially reversed Aβ toxicity, shown by an increase in the percentage of MTT reduction. In general, the MTT results agreed well with those from other assays. The control peptides C1 and C2 had no effect nor did iAβ5p. PPI-1019 successfully reduced Aβ toxicity. Some round-1 inhibitors had a weak beneficial effect, which was improved by some round-2 inhibitors. Round-3 inhibitors were the most effective, especially SEN303 and SEN304. Data for the 400 series of non-N-methylated peptides show that most have some toxicity in isolation, in contrast to all of the N-methylated peptides, which were always nontoxic (Figure F in the Supporting Information). SEN401 is the non-N-methylated analogue of SEN304, and it was similarly active, despite its toxicity.

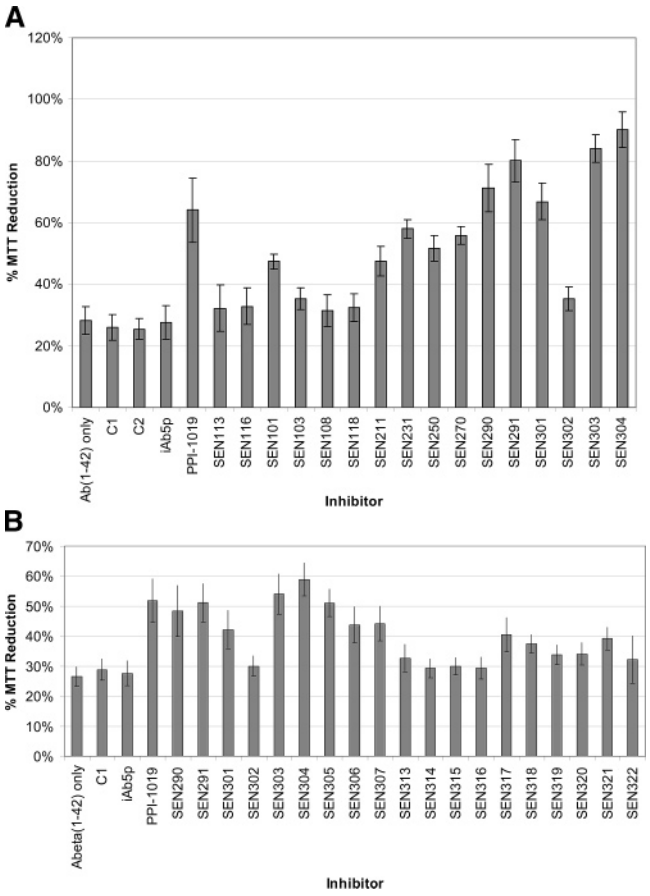

FIGURE 8: MTT toxicity. (A) Screened at 1:1 [10 μM inhibitors versus 10 μM Aβ(1−42)]. (B) Screened at 0.5:1 [5 μM inhibitors versus 10 μM Aβ(1−42)].

DISCUSSION

Our initial inhibitor was a core amyloidogenic fragment from the full-length Aβ, namely, L-Ac-[KLVFF]-NH_2. After four rounds of optimization, we reached a series of compounds with much higher activity, with SEN304 (D-[H-[(chGly)-(Tyr)-(chGly)-(chGly)-(mLeu)]-NH_2]) being the most effective inhibitor. Every side chain was thus changed from the starting compound, and the chirality was inverted. It is not clear why the D peptide should be more effective against an L peptide target, but similar results have been reported by other groups (*33*). This may be a general result, because Dzwolak et al. reported that mixtures of L- and D-polylysine formed more stable β sheets than the pure L or D peptides (*34*). The 400 series of inhibitors were designed to probe the effect of N-methylation on activity. They proved to be very difficult to work with, however, because of the low solubility, and were often toxic. We can conclude that a single *N*-methyl group greatly increases aqueous solubility, in agreement with previous work (*27*), and reduces inhibitor toxicity, even if its effect on inhibitor efficacy is difficult to assess. Only a single *N*-methyl group is necessary, and there was little or no gain in activity from multiple N-methylation.

Compounds were optimized primarily using the affinity and ThT data. These results correlated well with reducing Aβ toxicity, as measured by the MTT assay. The affinity assay gave data that correlated with ThT binding within a series of similar compounds, such as when just one side chain was altered. When large multiple changes were made, such as acetylation, changing chirality, and changing side chains, the results were more difficult to interpret. While the affinity assay is attractive, because dozens of compounds can be accurately measured in a day without using any Aβ, its results need to be interpreted cautiously. EM was less useful, because while some inhibitors did reduce or abolish fibril formation, others altered fibril morphology. How these EM data relate to toxicity is unclear. Our primary toxicity assay was MTT with PC12 cells, because it gave reproducible data at low concentrations and is widely used to assay Aβ toxicity.

We verified it by a comparison with other toxicity assays and a different cell line. It was reassuring, however, that the results from all of the assays correlated well and we were able to achieve significant increases in efficacy with each round. In addition, while the compounds were optimized primarily using the affinity and ThT data, these results paralleled with reducing Aβ toxicity, as measured by the MTT assay.

The best inhibitors never gave less than a 40% signal with the ThT assay, even if toxicity was reduced much below this in cell-based assays, while EM often showed a change in fibril morphology, rather than complete inhibition of fibril formation. We suggest that many inhibitors, including notably SEN304, may act by causing toxic Aβ oligomers to aggregate into nontoxic fibrils that weakly bind ThT. One concern at the start of this project was that if inhibitors compete for binding to aggregating Aβ with the wild-type peptide, they may increase the oligomer population, thus increasing toxicity. One could imagine that inhibitors could bind to both sides of a growing β sheet, blocking further aggregation and keeping the Aβ in an oligomeric form. Indeed, any interference with Aβ aggregation could increase the amount in shorter, more toxic forms. Reassuringly, no significant increase in toxicity was found with any N-methylated peptide inhibitor. Toxicity problems were only encountered with the rare cases when the inhibitors were toxic in isolation, as shown within the non-N-methylated round-4 library. Further work is clearly needed on the mode of action of the inhibitors.

It was also unclear whether inhibitors should be targeted at Aβ(1−40) or Aβ(1−42). While Aβ(1−40) is 10 times more abundant than Aβ(1−42) in vivo, Aβ(1−42) is more toxic. We addressed this by often assaying inhibitors against both target peptides. The results correlated very well, suggesting that optimizing the inhibitor structure against either target is acceptable. This may be because the binding site for an inhibitor is common to both target peptides.

In conclusion, we have found that N-methylated peptides can be powerful inhibitors of Aβ toxicity in vitro. Our best compounds had a higher activity than previously reported peptides, although D-[(mL)VFFL]-NH_2 (*29*) was also effective. We found no activity for Ac-[LPFFD]-NH_2 (*15*), with repeated measurements using a range of assays, despite previous reports. This may be because incorporating a Pro group prevents the adoption of the β conformation required for binding.

ACKNOWLEDGMENT

We thank Mark Treherne, David Scopes, and Omar El-Agnaf for helpful discussions.

SUPPORTING INFORMATION AVAILABLE

Figure A, aggregation kinetics of Aβ(1−40) and Aβ(1−42) with and without selected round-1 inhibitors; Figure B, initial round ThT assay; Figure C, round-1 ThT assay; Figure D, Aβ(1−40) versus Aβ(1−42) reversal; Figure E, Aβ(1−40) inhibition by ThT versus Aβ-binding affinity; Figure F, MTT toxicity assay for round-4 inhibitors. This material is available free of charge via the Internet at http://pubs.acs.org.

REFERENCES

1. Dobson, C. M. (1999) Protein misfolding, evolution and disease, *Trends Biochem. Sci. 24*, 329−332.
2. Holtzman, D. M., and Mobley, W. C. (1991) Molecular studies in Alzheimer's disease, *Trends Biochem. Sci. 16*, 140−144.
3. Selkoe, D. J. (1999) Translating cell biology into therapeutic advances in Alzheimer's disease, *Nature Suppl. 399*, A23−A31.
4. Robinson, S., and Bishop, G. (2002) Aβ as a bioflocculant: Implications for the amyloid hypothesis of Alzheimer's disease, *Neurobiol. Aging 23*, 1051−1072.
5. Klein, W. L., Krafft, G. A., and Finch, C. E. (2001) Targeting small A βoligomers: The solution to an Alzheimer's disease conundrum? *Trends Neurosci. 24*, 219−224.
6. Lambert, M. P., Barlow, A. K., Chromy, B. A., Edwards, C., Freed, R., Liosatos, M., Morgan, T. E., Rozovsky, I., Trommer, B., Viola, K. L., Wals, P., Zhang, C., Finch, C. E., Krafft, G. A., and Klein, W. L. (1998) Diffusible, nonfibrillar ligands derived from Aβ1−42 are potent central nervous system neurotoxins, *Proc. Nat. Acad. Sci. U.S.A. 95*, 6448−6453.
7. de Felice, F. G., and Ferreira, S. T. (2002) β-Amyloid production, aggregation, and clearance as targets for therapy in Alzheimer's disease, *Cell Mol. Neurobiol. 22*, 545−563.
8. Conway, K. A., Baxter, E. W., Felsenstein, K. M., and Reitz, A. B. (2003) Emerging β-amyloid therapies for the treatment of Alzheimer's disease, *Curr. Pharm. Des. 6*, 427−447.
9. Lahiri, D. K., Farlow, M. R., Sambamurti, K., Greig, N. H., Giacobini, E., and Schneider, L. S. (2003) A critical analysis of new molecular targets and strategies for drug developments in Alzheimer's disease, *Curr. Drug Targets 4*, 97−112.
10. Haass, C., and de Strooper, B. (1999) The presenilins in Alzheimer's disease—Proteolysis holds the key, *Science 286*, 916−919.
11. Lansbury, P. T. J. (1997) Inhibition of amyloid formation: A strategy to delay the onset of Alzheimer's disease, *Curr. Opin. Struct. Biol. 1*, 260−267.
12. Mason, J. M., Kokkoni, N., Stott, K., and Doig, A. J. (2003) Design strategies for anti-amyloid agents, *Curr. Opin. Struct. Biol. 13*, 526−532.
13. Tjernberg, L. O., Näslund, J., Lindqvist, F., Johansson, J., Karlström, A. R., Thyberg, J., Terenius, L., and Nordstedt, C. (1996) Arrest of β-amyloid fibril formation by a pentapeptide ligand, *J. Biol. Chem. 271*, 8545−8548.
14. Soto, C., Kindy, M. S., Baumann, M., and Frangione, B. (1996) Inhibition of Alzheimer's amyloidosis by peptides that prevent β-sheet conformation, *Biochem. Biophys. Res. Comm. 226*, 672−680.
15. Poduslo, J. F., Curran, G. L., Kumar, A., Frangione, B., and Soto, C. (1999) β-Sheet breaker peptide inhibitor of Alzheimer's amyloidogenesis with increased blood-brain barrier permeability and resistance to proteolytic degradation in plasma, *J. Neurobiol. 39*, 371−382.
16. Soto, C., Sigurdsson, E. M., Morelli, L., Kumar, R. A., Castaño, E. M., and Frangione, B. (1998) β-Sheet breaker peptides inhibit fibrillogenesis in a rat brain model of amyloidosis: Implications for Alzheimer's therapy, *Nat. Med. 4*, 822−826.
17. Ghanta, J., Shen, C. L., Kiessling, L. L., and Murphy, R. M. (1996) A strategy for designing inhibitors of β-amyloid toxicity, *J. Biol. Chem. 271*, 29525−29528.
18. Pallitto, M. M., Ghanta, J., Heinzelman, P., Kiessling, L. L., and Murphy, R. M. (1999) Recognition sequence design for peptidyl modulators of β-amyloid aggregation and toxicity, *Biochemistry 38*, 3570−3578.
19. Lowe, T. L., Strzelec, A., Kiessling, L. L., and Murphy, R. M. (2001) Structure−function relationships for inhibitors of β-amyloid toxicity containing the recognition sequence KLVFF, *Biochemistry 40*, 7882−7889.
20. Sato, T., Kienlen-Campard, P., Ahmed, M., Liu, W., Li, H. L., Elliott, J. I., Aimoto, S., Constantinescu, S. N., Octave, J. N., and Smith, S. O. (2006) Inhibitors of amyloid toxicity based on β-sheet packing of Aβ40 and Aβϵτα42, *Biochemistry 45*, 5503−5516.
21. Yang, F., Lim, G. P., Begum, A. N., Ubeda, O. J., Simmons, M. R., Ambegaokar, S. S., Chen, P. P., Kayed, R., Glabe, C. G., Frautschy|, S. A., and Cole, G. M. (2005) Curcumin inhibits formation of amyloid oligomers and fibrils, binds plaques, and reduces amyloid in vivo, *J. Biol. Chem. 280*, 5892−5901.
22. Torok, M., Abid, M., Mhadgut, S. C., and Torok, B. (2006) Organofluorine inhibitors of amyloid fibrillogenesis, *Biochemistry 45*, 5377−5383.
23. Cohen, T., Frydman-Marom, A., Rechter, M., and Gazit, E. (2006) Inhibition of amyloid fibril formation and cytotoxicity by hydroxyindole derivatives, *Biochemistry 45*, 4727−4735.
24. Rijkers, D. T. S., Hoppener, J. W. M., Posthuma, G., Lips, C. J. M., and Liskamp, R. M. J. (2002) Inhibition of amyloid fibril

formation of human amylin by N-alkylated amino acid and α-hydroxy acid residue containing peptides, *Chem.—Eur. J.* 4285−4291.
25. Hughes, E., Burke, R. M., and Doig, A. J. (2000) Inhibition of toxicity in β-amyloid peptide fragment β(25−35) using N-methylated derivatives—A general strategy to prevent amyloid formation, *J. Biol. Chem. 275*, 25109−25515.
26. Gordon, D. J., Sciaretta, K. L., and Meredith, S. C. (2001) Inhibition of β-amyloid(40) fibrillogenesis and disassembly of β-amyloid(40) fibrils by short β-amyloid cogeners containing *N*-methyl amino acids at alternate residues, *Biochemistry 40*, 8237−8245.
27. Gordon, D. J., Tappe, R., and Meredith, S. C. (2002) Design and characterization of a membrane permeable *N*-methyl amino acid-containing peptide that inhibits Aβ(1−40) fibrillogenesis, *J. Pept. Res. 60*, 37−55.
28. Cruz, M., Tusell, J. M., Grillo-Bosch, D., Albericio, F., Serratosa, J., Rabanal, F., and Girault, E. (2004) Inhibition of β-amyloid toxicity by short peptides containing *N*-methyl amino acids, *J. Pept. Res. 63*, 324−328.
29. Zagorski, M. G., Yang, J., Shao, H., Ma, K., Zeng, H., and Hong, A. (1999) Methodological and chemical factors affecting amyloid β-peptide amyloidogenicity, *Methods Enzymol. 309*, 189−203.
30. LeVine, H. (1993) Thioflavine T interaction with synthetic Alzheimer's disease β-amyloid peptides: Detection of amyloid aggregation in solution, *Protein Sci. 2*, 404−410.
31. Shearman, M. S., Ragan, C. I., and Iversen, L. L. (1994) Inhibition of PC12 cell redox activity is a specific, early indicator of the mechanism of β-amyloid mediated cell death, *Proc. Nat. Acad. Sci. U.S.A. 91*, 1470−1474.
32. Findeis, M. A., Musso, G. M., Arico-Muendel, C. C., Benjamin, H. W., Hundal, A. M., Lee, J.-J., Chin, J., Kelley, M., Wakefield, J., Hayward, N. J., and Molineaux, S. M. (1999) Modified-peptide inhibitors of amyloid β-peptide polymerization, *Biochemistry 38*, 6791−6800.
33. Chalifour, R. J., McLaughlin, R. W., Lavoie, L., Morisette, C., Tremblay, N., Boule, M., Sarazin, P., Stea, D., Lacombe, D., Tremblay, P., and Gervais, F. (2003) Stereoselective interactions of peptide inhibitors with the β-amyloid peptide, *J. Biol. Chem. 278*, 34874−34881.
34. Dzwolak, W., Ravindra, R., Nicolini, C., Ralf Jansen, R., and Winter, R. (2004) The diastereomeric assembly of polylysine is the low-volume pathway for preferential formation of β-sheet aggregates, *J. Am. Chem. Soc. 126*, 3762−3768.

BI060837S